

Investigation of organelle-specific intracellular water structures with Raman microspectroscopy

Shraeddha Tiwari,^a Masahiro Ando^a and Hiro-o Hamaguchi^{a,b*}

The study of intracellular water in living cells is a challenge of fundamental importance. While the critical roles of water in maintaining and propagating life have been widely recognized and accepted, our understanding of water/biomolecule interactions is surprisingly limited. Using Raman microspectroscopic imaging of a living yeast cell followed by a multivariate analysis in form of the nonnegative matrix factorization method, we successfully resolve organelle-specific water structures. The intensities and the band profiles of the segregated water OH stretch spectra yield important and otherwise unobtainable information on the extensive effect of the water/biomolecule interactions in a given organelle on the hydrogen-bonding network of water molecules. Copyright © 2012 John Wiley & Sons, Ltd.

Supporting information may be found in the online version of this article.

Keywords: Raman microspectroscopy; water; living cells; imaging; multivariate analysis

Life, as we know it, cannot exist without water.^[1–3] Physiological processes ranging from cell division^[4] and osmotic stress response^[5] to carcinogenesis^[6] have been attributed to intracellular hydration, which eventually leads to the hypothesis of intracellular water networks (also known as 'biological water').^[7] Water molecules inside a living cell are believed to have structural and chemical properties that are distinct from those of bulk water. It is now known that the water molecules in the vicinity of a biomolecule, e.g. on the surface of a protein molecule, form a characteristic network which differs substantially from bulk water.^[8–10] However, the extension of such studies from *in vitro* solutions to living cells has been challenging. For example, the results based on NMR T_1 relaxation times in mitotic HeLa cells have been contradictory^[11,12] while inelastic incoherent neutron scattering studies cannot be extended from the model systems to living cells.^[13] Such ambiguities are inevitable since most of the techniques used to study aqueous biomolecular solutions are either incompatible with living cell studies or are incapable of providing label-free detection with adequate spatial and temporal resolution.

The problem has been solved with the use of Raman microspectroscopy, which is compatible with living cell measurements and can provide time- and space-resolved molecular information without the need for any pretreatment.^[14–16] The contour of the OH stretch Raman band of water is known to be sensitive to the changes in the hydrogen-bonding networks.^[17,18] It can be modeled as a continuum representing hydrogen-bonding energy and geometry distributions,^[19] making it an ideal candidate to probe interactions among intracellular water molecules.

In the present report, we employ Raman microspectroscopy as the experimental method coupled with nonnegative matrix factorization (NMF) to study the intracellular water molecules in living yeast cells (diploid *S. cerevisiae*). The NMF analysis of the OH stretch region (from 3100 cm^{-1} to 3800 cm^{-1}) for a typical diploid *S. cerevisiae* yeast cell resulted in the resolution of five

spectral components, labeled C1 to C5. (See Supporting Information for experimental and analysis details) and rearranged as per the spatial coordinates of imaging (Fig. 1). The well-defined spatial distributions of the five components in the pseudocolour images of H matrix are almost mutually exclusive, indicating that the resolved components represent physically meaningful spatial distributions. The most plausible explanation for such well-defined spatial distributions is that the differences in the hydrogen-bonding network of water are differentiated by the multivariate NMF analysis. The results are particularly encouraging since none of the earlier reports employing vibrational spectroscopy for studying intracellular water could resolve the intracellular OH band profile to reveal such specific spatial distributions inside living cells.^[20,21]

The average spectra for each of the components C1 to C5 (calculated by employing the coefficients of the H matrix^[22]) in Fig. 1 show the relative intensities of the OH stretch bands for the resolved components. The C5 component has a relatively lower intensity in the lower wavenumber OH stretch region (3200 cm^{-1}) as compared to the intensity in the 3400 cm^{-1} region (I_{3400}/I_{3230} is 0.73 for C5 as compared to 0.82 for C1) indicating a lower proportion of stable hydrogen-bonding network in component C5 than in bulk water,^[19] showing that it originates from an intracellular region with significantly disrupted hydrogen-bonding interactions.

* Correspondence to: Hiro-o Hamaguchi, Department of Chemistry, School of Science, The University of Tokyo, Tokyo, Japan. E-mail: hhama@chem.s.u-tokyo.ac.jp

a Department of Chemistry, School of Science, The University of Tokyo, Tokyo, Japan

b Department of Applied Chemistry and Institute of Molecular Science, National Chiao Tung University, Hsinchu, Taiwan

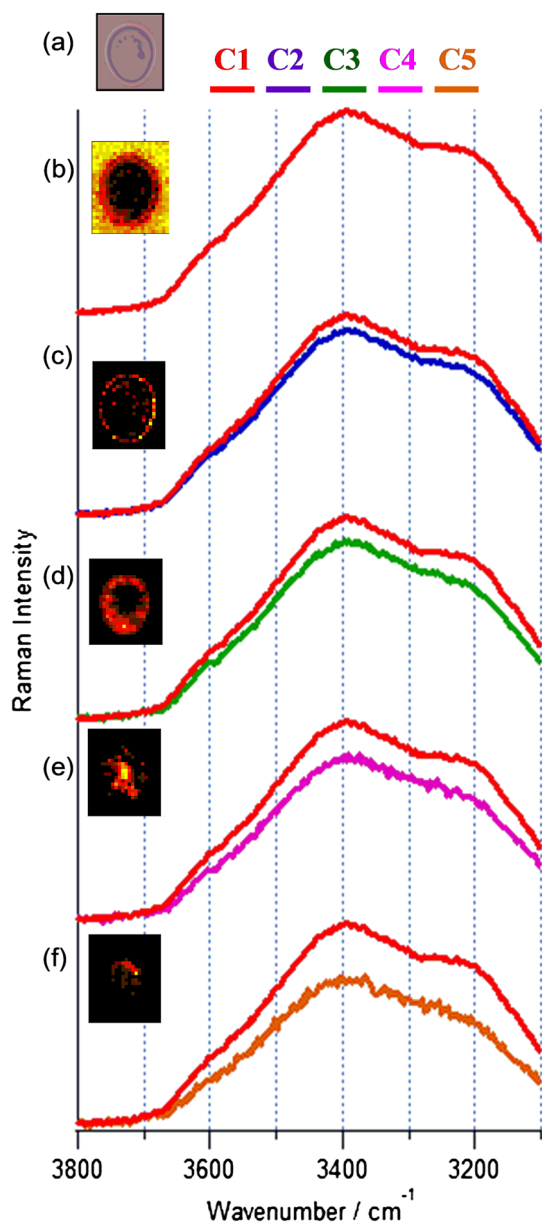


Figure 1. NMF analysis of the OH stretch Raman band. (a) Optical image of the yeast cell chosen for Raman imaging. The spatial coefficients obtained from the H matrix (rearranged according to spatial coordinates to generate pseudocolour Raman images) and the average spectra in the 3100 to 3800 cm^{-1} region, representing the components C1 to C5 (determined from the clustering of the original data based on the coefficients in the H matrix) - (b) component C1; (c) component C2; (d) component C3; (e) component C4 and (f) component C5. The average spectra for components C2 - C5 superimposed with the average spectrum for C1 component (bulk water spectrum depicted in red) for comparison.

The lack of consensus associated with the spectral assignment of the OH stretch region in aqueous solutions in the past^[23] and limited knowledge of actual water structures in living cells impedes further interpretation of the results. In order to overcome this difficulty, information from the fingerprint region (400 to 1800 cm^{-1}) is highly useful. It is observed that the average spectrum corresponding to each provides critical information on the molecular composition corresponding to each component (Fig. 2).

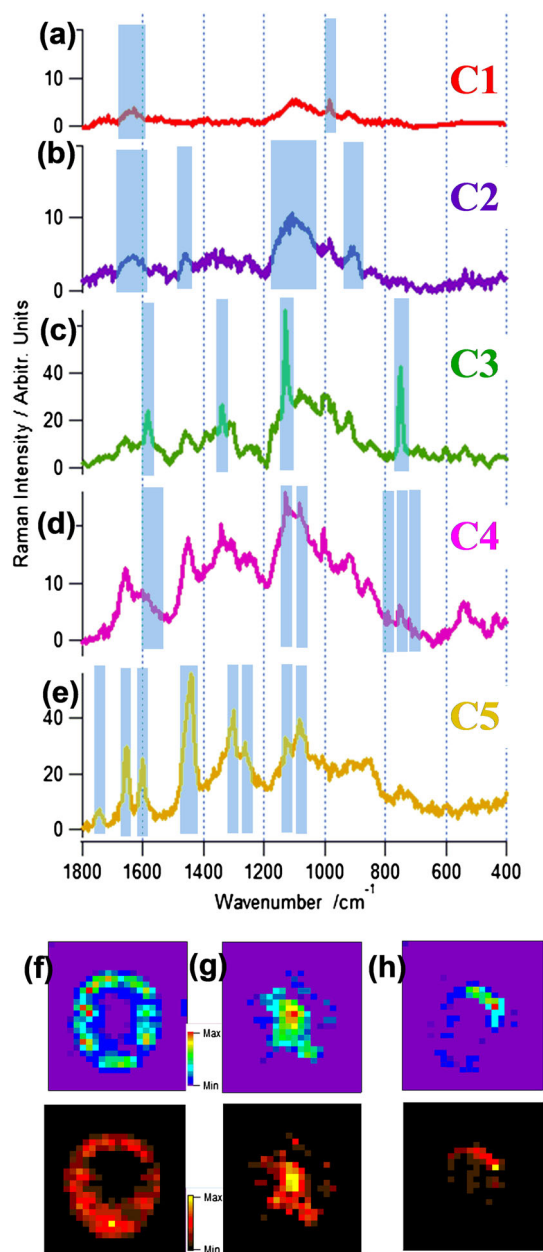


Figure 2. Identification of resolved components: (a-e) Average fingerprint region spectra (400 to 1800 cm^{-1}), representing the components C1 to C5. The average spectra are determined from the clustering of the original data based on the coefficients in the H matrix. (f) Univariate Raman mapping of the 1584 cm^{-1} resonance Raman band of cytochrome C3 (top), compared to the pseudocolour image of C3 (bottom). (g) Univariate Raman mapping of the 720 cm^{-1} band of nucleic acids (top), compared to the pseudocolour image of C4 (bottom). (h) Correspondence between the univariate Raman mapping of the 1744 cm^{-1} band from phospholipid esters (top) and the pseudocolour image of component C5 (bottom).

The average fingerprint spectrum corresponding to the C1 component consists of no major Raman peaks except for a weak Raman signals at 1630 cm^{-1} (ν_2 bending mode of water) and 980 cm^{-1} (phosphate), thus confirming that component C1 originates exclusively from the bulk water in the extracellular region. In the C2 average fingerprint spectrum, a broad Raman peak at 890 cm^{-1} (CO stretch of glycosides), a feature signal between 1050 and 1150 cm^{-1} (terminal CH bend of reducing pyranose rings) and a band at 1462 cm^{-1} (terminal CH bend of

nonreducing pyranose rings) are observed indicating that the C2 component originates primarily from the cell wall. Since the yeast cell wall makes up 25% of the dry matter and contains more than 85% of the total carbohydrates in the cell, the C2 OH stretch signal can be assumed to originate from the carbohydrate OH-stretch in addition to the water molecules in the vicinity. Despite this fact, a multi-component fitting analysis of a typical cell wall spectrum with standard spectra for water, glucan and mannan indicates that the contribution of water is more than 90% of the total intensity in the OH stretch region as shown in Fig.S1 (Supporting Information).

The average fingerprint spectrum representing the component C3 shows sharp Raman peaks at 1584, 1315, 1129 and 749 cm^{-1} – the resonance-enhanced Raman bands from different cytochrome species at 532-nm excitation.^[24–26] Since the cytochromes are widely distributed throughout the cytoplasm in general and mitochondria in particular, it can be concluded that the cytoplasmic OH stretch has been successfully segregated, as further verified by the close correspondence between the pseudocolour map for C3 and the univariate Raman image for the low-spin heme band at 1584 cm^{-1} (Fig. 2f).

The average fingerprint spectrum for the component C4 contains Raman bands associated with proteins such as 1665 – 1660 cm^{-1} (amide I), 1250 – 1300 cm^{-1} (amide III) and 1003 cm^{-1} (phenylalanine residue). In addition, Raman bands of nucleic acids including 728 cm^{-1} (dA), 750 cm^{-1} (dT), 781, 1093 and 1129 cm^{-1} (backbone OPO str.), 1376 cm^{-1} (T, A) and 1576 cm^{-1} (dA and dG ring) are also observed,^[15] clearly demonstrating the successful differentiation by the NMF analysis of the OH signal in the nuclear region. The univariate Raman mapping of the 728 cm^{-1} band is identical to the pseudocolour image of the component C4 (Fig. 2g).

Finally, the fingerprint spectrum obtained from the coefficients for the component C5 consists of Raman bands from typical phospholipids (1062, 1122, 1266, 1303, 1440 and 1744 cm^{-1}).^[15] The univariate mapping of 1744 cm^{-1} band overlaps perfectly with the spatial distribution of C5 (Fig. 2h), confirming that C5 originates exclusively from water molecules around phospholipid-rich organelles like lipid bodies. The identification of components corresponding to the extracellular region (C1), cell wall (C2), cytoplasm (C3), nucleus (C4) and lipid-rich region (C5) establishes their physical relevance in terms of the organelle-specific water structure. It also provides a basis for explaining the variation in band profiles of the isolated components. For example, lower number of stable hydrogen bonding interactions and much lower concentration of water molecules (C5 in Fig. 1) are consistent with the assignment of C5 to water molecules in lipid rich organelles such as lipid bodies. Water molecules trapped in multilamellar vesicle had greater orientation disorder, resulting in a relative decrease in intensity in the 3240 cm^{-1} region as compared to the 3440 cm^{-1} region.^[27] The lipid – water interactions impose orientational and density constraints on the strength of hydrogen bond, resulting in weaker water–water interactions.^[28]

To summarize, we have successfully established the existence of organelle-specific water structures in living yeast cells using a

combination of Raman microspectroscopic imaging and a multivariate analysis. The results provide direct evidence for the existence of ‘biological water’ in living cells, indicating how the water hydrogen-bonding network is likely to provide a highly sensitive and extensive means of bio-regulation.

Acknowledgement

The authors thank Mr. Hirokazu Minami (Python) for the development of NMF software.

Supporting information

Supporting information may be found in the online version of this article.

References

- [1] M. Chaplin, *Nat. Rev. Mol. Cell Biol.* **2006**, *7*, 861.
- [2] P. Ball, *Chem. Rev.* **2008**, *108*, 74.
- [3] P. Wiggins, *PLoS One* **2008**, *3*, e1406.
- [4] E. A. Kadyshovich, V. E. Ostrovskii, *Thermochim. Acta* **2007**, *458*, 148.
- [5] G. D. Fullerton, K. M. Kanal, I. L. Cameron, *Cell Biol. Int.* **2006**, *30*, 74.
- [6] G. I. McIntyre, *Med. Hypotheses* **2006**, *66*, 518.
- [7] Z. Szolnoki, *Biochem. Biophys. Res. Commun.* **2007**, *357*, 331.
- [8] R. Pethig, *Annu. Rev. Phys. Chem.* **1992**, *43*, 177.
- [9] S. K. Pal, J. Peon, B. Bagchi, A. H. Zewail, *J. Phys. Chem. B* **2002**, *106*, 12376.
- [10] U. Heugen, G. Schwaab, E. Bründermann, M. Heyden, X. Yu, D. M. Leitner, M. Havenith, *Proc. Natl. Acad. Sci. U.S.A.* **2006**, *103*, 12301.
- [11] P. T. Beall, C. F. Hazlewood, P. N. Rao, *Science* **1976**, *192*, 904.
- [12] D. N. Wheatley, M. S. Inglis, M. A. Foster, J. E. Rimington, *J. Cell Sci.* **1987**, *88*, 13.
- [13] S. V. Ruffe, I. Michalarias, J.-C. Li, R. C. Ford, *J. Am. Chem. Soc.* **2002**, *124*, 565.
- [14] W. E. Huang, M. Li, R. M. Jarvis, R. Goodacre, S. A. Banwart, *Adv. Appl. Microbiol.*, **2010**, *70*, 153.
- [15] Y.-S. Huang, T. Karashima, M. Yamamoto, H. Hamaguchi, *Biochemistry* **2005**, *44*, 10009.
- [16] C.-K. Huang, H. Hamaguchi, S. Shigeto, *Chem. Commun.* **2011**, *47*, 9423.
- [17] Y. Maeda, M. Ide, H. Kitnao, *J. Mol. Liq.* **1999**, *80*, 149.
- [18] S. A. Corcelli, J. L. Skinner, *J. Phys. Chem. A* **2005**, *109*, 6154.
- [19] J. D. Smith, C. D. Cappa, K. R. Wilson, R. C. Cohen, P. L. Geissler, R. J. Saykally, *Proc. Natl. Acad. Sci. U.S.A.* **2005**, *102*, 14171.
- [20] J. L. Dashnau, L. K. Conlin, H. C. M. Nelson, J. M. Vanderkooi, *Biochim. Biophys. Acta* **2008**, *1780*, 41.
- [21] J. Dong, J. Malsam, J. C. Bischof, A. Hubel, A. Aksan, *Biophys. J.* **2010**, *99*, 2453.
- [22] J.-P. Brunet, P. Tamayo, T. R. Golub, J. P. Mesirov, *Proc. Natl. Acad. Sci. U.S.A.* **2004**, *101*, 4164.
- [23] S. Gopalakrishnan, D. Liu, H. C. Allen, M. Kuo, M. J. Shultz, *Chem. Rev.* **2006**, *106*, 1155.
- [24] K. Hamada, K. Fujita, N. I. Smith, M. Kobayashi, Y. Inouye, S. Kawata, *J. Biomed. Opt.* **2008**, *13*, 044027.
- [25] C. Onogi, H. Hamaguchi, *Chem. Lett.* **2010**, *39*, 270.
- [26] M. Kakita, V. Kaliaperumal, H. Hamaguchi, *J. Biophotonics* **2012**, *5*, 20.
- [27] M. Lafleur, M. Pigeon, M. Pezolet, J. P. Caille, *J. Phys. Chem.* **1989**, *93*, 1522.
- [28] Z. Arsov, M. Rappolt, J. Grdadolnik, *Chemphyschem* **2009**, *10*, 1438.